

## Supporting Information

### **Rationally tuning atomic ratio of electrodeposited NiP for greatly enhanced hydrogen evolution in alkaline media**

Qian Liu,<sup>a,c</sup> Chun Tang,<sup>a,c</sup> Shiyu Lu,<sup>a,c</sup> Zhuo Zou,<sup>a,c</sup> Shuang Gu,<sup>a,c</sup> Yuhuan Zhang,<sup>a,c</sup>  
and Chang Ming Li<sup>\*a,b,c</sup>

<sup>a</sup>Institute for Clean Energy & Advanced Materials (ICEAM), Southwest University, Chongqing 400715, P.R. China

<sup>b</sup>Institute for Materials Science and Devices, Suzhou University of Science and Technology, Suzhou 215009, P.R. China

<sup>c</sup>Chongqing Key Laboratory for Advanced Materials and Technologies of Clean Energy, Chongqing 400715, P.R. China

†E-mail: [ecmli@swu.edu.cn](mailto:ecmli@swu.edu.cn) (Chang Ming Li)

#### **Experimental Section**

**Materials:** Ni(SO<sub>4</sub>)<sub>2</sub>·6H<sub>2</sub>O, KOH and NaH<sub>2</sub>PO<sub>2</sub> were purchased from Aladdin Industrial Corporation. HCl, H<sub>2</sub>SO<sub>4</sub>, NaAc·3H<sub>2</sub>O and absolute ethyl alcohol were bought from Sinopharm Chemical Reagent Co., Ltd. All chemicals were used as received without further purification. Deionized water (18.2 MΩ, 25 °C) used throughout all experiment was obtained from a Milli-Q Plus water purification system (Millipore).

**Preparation of metallic Ni on Ti:** A three-electrode configure was used for the electrodeposition. The electrolyte was prepared by dissolving 0.7885 g

$\text{Ni}(\text{SO}_4)_2 \cdot 6\text{H}_2\text{O}$  and 0.8165 g  $\text{NaOA} \cdot 3\text{H}_2\text{O}$  in 30 mL deionized water. Then the pH of this solution was adjusted to 2.0 ~ 2.5 by using concentrated  $\text{H}_2\text{SO}_4$ . A piece of titanium plate, a saturated calomel electrode (SCE), and a piece of platinum plate were used as work, reference and counter electrode, respectively. Before electrodeposition, the titanium plate was pretreated by immersing in concentrated HCl for 30 min at 60 °C. The titanium plate washed with deionized water and ethanol for several times and dried under room temperature. The electrodeposition was conducted on a CHI 760e electrochemical workstation (CH Instrument, Shanghai, China) by amperometric technology at -1.0 V for 2000s. The loading of the obtained Ni on Ti plate is 3.12 mg  $\text{cm}^{-2}$ .

**Preparation of  $\text{Ni}_x\text{P}_y$  samples on Ti:** The electrolyte was prepared by the following steps: first, 0.2639 g  $\text{NaH}_2\text{PO}_2$  and 0.8165 g  $\text{NaOA} \cdot 3\text{H}_2\text{O}$  were dissolved in 30 mL deionized water and the pH value of the solution was adjusted by a certain amount of concentrated  $\text{H}_2\text{SO}_4$  or 1.0 M KOH. Then 0.7885g  $\text{Ni}(\text{SO}_4)_2 \cdot 6\text{H}_2\text{O}$  was added to the solution. For preparation of  $\text{Ni}_{94}\text{P}_6$ , 50  $\mu\text{L}$  1.0 M KOH was adding into the above solution. For preparation of  $\text{Ni}_{90}\text{P}_{10}$ ,  $\text{Ni}_{82}\text{P}_{18}$ , and  $\text{Ni}_{75}\text{P}_{25}$ , the amount of concentrated  $\text{H}_2\text{SO}_4$  were 0, 65, and 195 mL, respectively. The electrodeposition was carried out at -1.0 V for 500, 500, 600 and 1600s to obtain  $\text{Ni}_{94}\text{P}_6$ ,  $\text{Ni}_{90}\text{P}_{10}$ ,  $\text{Ni}_{82}\text{P}_{18}$ , and  $\text{Ni}_{75}\text{P}_{25}$ , and loadings of them are 3.31, 3.25, 3.10 and 3.19 mg  $\text{cm}^{-2}$ , respectively.

**Characterizations:** SEM measurements were made on a field-emission scanning electron microscope (FESEM; JEOL-6300F) at an accelerating voltage of 20 kV. XRD data were collected using a RigakuD/MAX 2550 diffractometer with Cu  $\text{K}\alpha$

radiation ( $\lambda=1.5418 \text{ \AA}$ ). X-ray photoelectron spectroscopy (XPS) data were collected in a ESCALAB 250Xi X-ray photoemission spectrometer. C 1s (284.80 eV) was used to align all the XPS peaks.

**Electrochemical measurements:** All electrochemical measurements were conducted in a typical three-electrode configure with an electrolyte solution of 1.0 M KOH, consisting of a work electrode, a SCE reference electrode, and a platinum plate counter electrode. Linear sweep voltammetry was carried out at a scan rate of 5 mV/s.

**Electrochemical surface area (ECSA):** According to the literature about the electrochemical surface area measurements in electrochemistry,<sup>1</sup> ECSA can be calculated by non-Faradic double-layer capacitance ( $C_{dl}$ ) ratio. The ratio is the  $C_{dl}$  of the prepared electrocatalyst to the specific capacitance ( $C_s$ ) of a standard flat electrode of 1 cm<sup>2</sup> real surface area. The general value of  $C_s$  is range from 20 to 60  $\mu\text{F cm}^{-2}$ . The average value of 40  $\mu\text{F cm}^{-2}$  is use in this work.<sup>2</sup> The  $C_{dl}$  of pure Ni, Ni<sub>94</sub>P<sub>6</sub>, Ni<sub>90</sub>P<sub>10</sub>, Ni<sub>82</sub>P<sub>18</sub>, and Ni<sub>75</sub>P<sub>25</sub> are 0.11, 0.38, 0.55, 0.12, 0.10 mF cm<sup>-2</sup>, respectively (Fig. S1). Thus the ECSA of them are 13.75, 9.5, 3, 2.75 and 2.5 cm<sup>2</sup>. For Ni<sub>90</sub>P<sub>10</sub> on 3D network structure CF, the ECSA (9.75 cm<sup>2</sup>) is obtained by the ratio of the  $C_{dl}$  of Ni<sub>90</sub>P<sub>10</sub>/CF to that of a bare CF.

**Computational Methods:** The Vienna ab initio simulation package (VASP) was used in all calculations in this study.<sup>3</sup> PBE functional<sup>4</sup> was applied for the exchange-correlation energy and projector augmented wave potentials<sup>5,6</sup>. The kinetic energy cutoff was set to 500 eV. The ionic relaxation was carried out until the force on each atom is less than 0.01 eV/Å. The k-points meshes sampling was based on the

Monkhorst-Pack method.<sup>7</sup> In order to minimize the undesired interactions between images, a vacuum of 15 Å was considered along the z axis. The lattice parameters of face-centered cubic structure of Ni was optimized to  $a = b = c = 3.5238$  Å. The structures of Ni<sub>x</sub>P<sub>y</sub> samples were obtained by substituting nickel atom within the unit cell with phosphorus atoms in all possible geometries and selected the most stable ones. Chemisorption was modeled on (111) surface of Ni and Ni<sub>x</sub>P<sub>y</sub>. The surfaces were constructed as slab consists of three layers within periodic boundary conditions, separated by a 15 Å vacuum layer. For these calculations, three layers with  $4 \times 4 \times 1$  k-point mesh was used for pure Ni and Ni<sub>x</sub>P<sub>y</sub>. It has been proved that the hydrogen evolution activity is closely correlated with the free energy of hydrogen to the electrocatalyst surface.<sup>8</sup> The equation, which is proposed by Norskov and coworkers, used to calculate the free energy change for H adsorption on both pure Ni and Ni<sub>x</sub>P<sub>y</sub> surfaces ( $\Delta G_H$ ) is:<sup>8</sup>

$$\Delta G_H = E_{\text{total}} - E_{\text{surface}} - E_{\text{H}_2} / 2 + \Delta E_{\text{ZPE}} - T\Delta S$$

where  $E_{\text{total}}$  is the total energy of the adsorption state,  $E_{\text{surface}}$  is the energy of the corresponding surface,  $E_{\text{H}_2}$  is the energy of H<sub>2</sub> in gas phase,  $\Delta E_{\text{ZPE}}$  is the zero-point energy change and  $\Delta S$  is the entropy change.

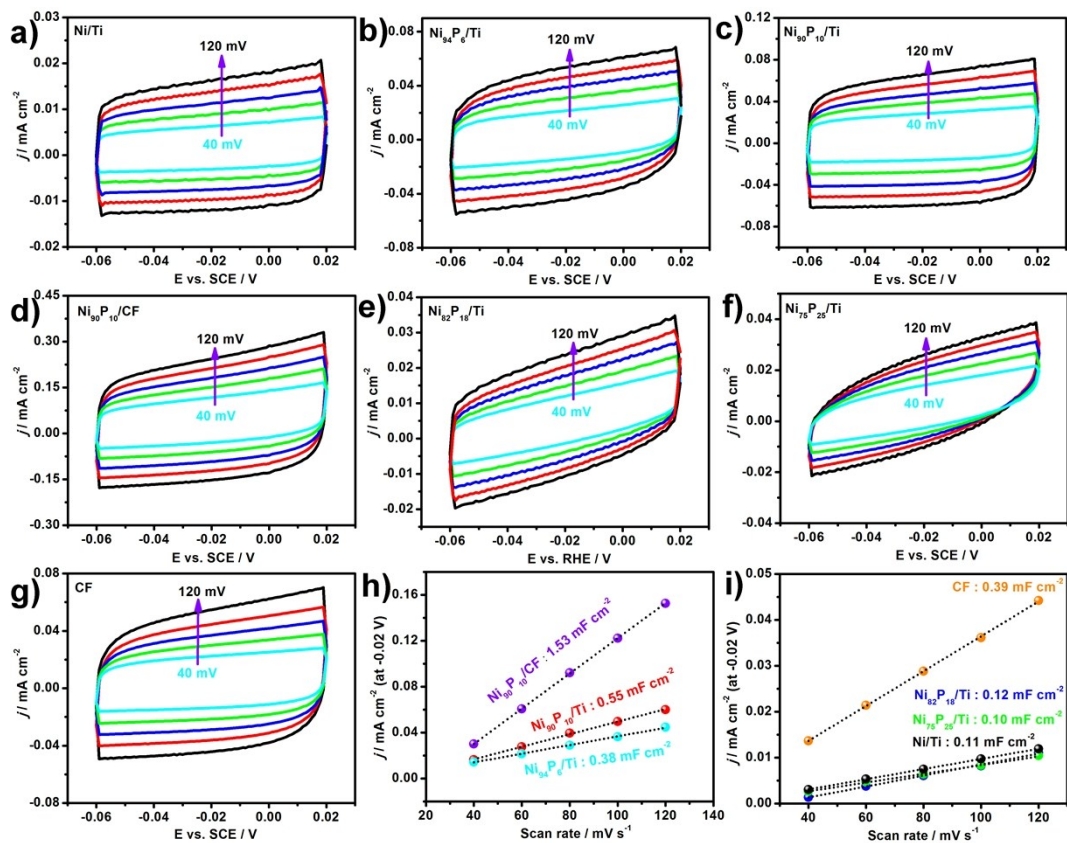


**Fig. S1** Cyclic voltammograms with scan rates of 40, 60, 80, 100, and 120 mV s<sup>-1</sup> for (a) Ni/Ti, (b) Ni<sub>94</sub>P<sub>6</sub>/Ti, (c) Ni<sub>90</sub>P<sub>10</sub>/Ti, (d) Ni<sub>90</sub>P<sub>10</sub>/CF, (e) Ni<sub>82</sub>P<sub>18</sub>/Ti, (f) Ni<sub>75</sub>P<sub>25</sub>/Ti and (g) bare CF. (h, i) The capacitive current densities at center potential of -0.02 V vs as a function of scan rate for them.

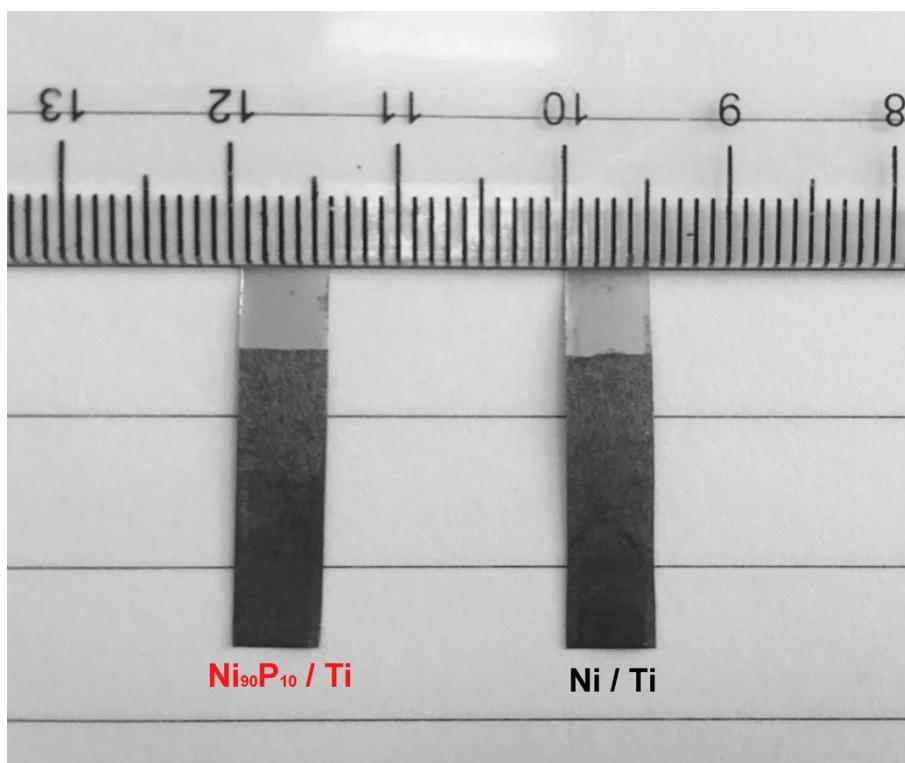


**Fig. S2** Optical photograph of Ni<sub>90</sub>P<sub>10</sub> and Ni micro-spheres on Ti plate, respectively.

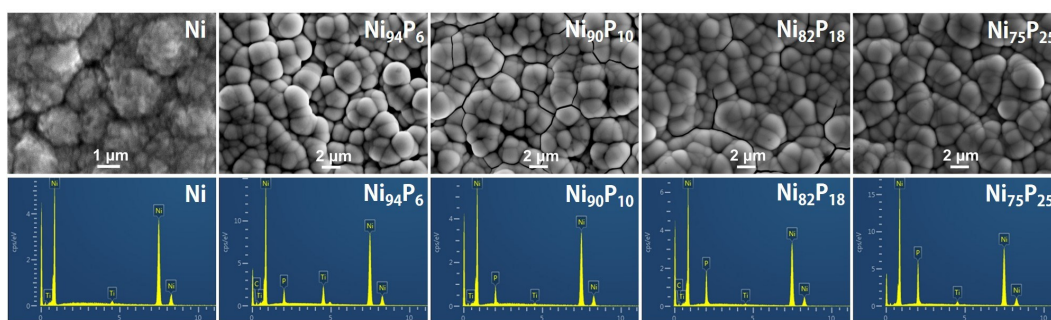


**Fig. S3** SEM images and the corresponding EDS spectra of Ni, Ni<sub>94</sub>P<sub>6</sub>, Ni<sub>90</sub>P<sub>10</sub>, Ni<sub>82</sub>P<sub>18</sub>, and Ni<sub>75</sub>P<sub>25</sub> micro-spheres on Ti plate.

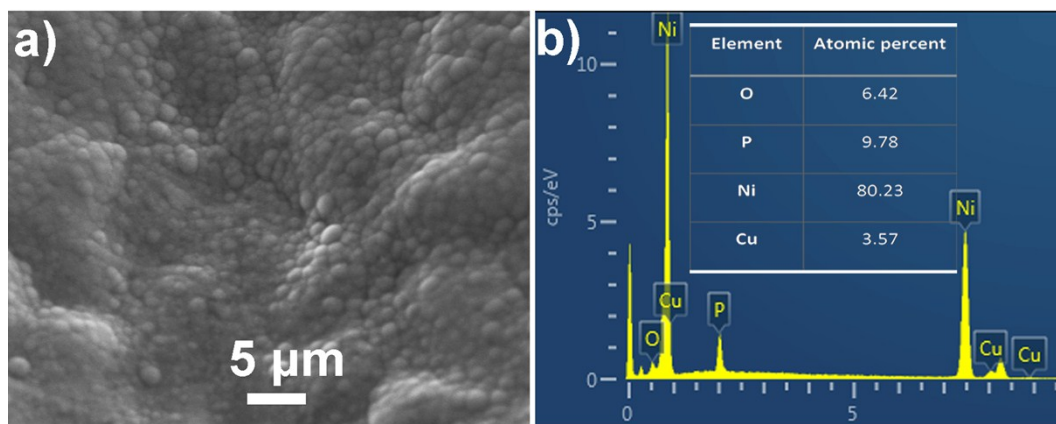


**Fig. S4** (a) SEM image and (b) the corresponding EDS spectrum of  $\text{Ni}_{90}\text{P}_{10}/\text{CF}$ .



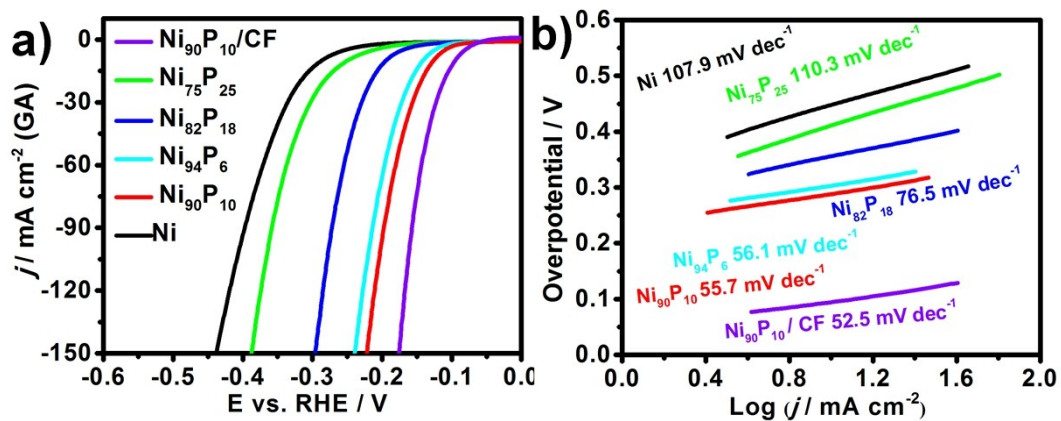


**Fig. S5** (a) LSV curves normalized by geometric area (GA) and (b) the corresponding Tafel plots for Ni, Ni<sub>94</sub>P<sub>6</sub>, Ni<sub>90</sub>P<sub>10</sub>, Ni<sub>82</sub>P<sub>18</sub>, and Ni<sub>75</sub>P<sub>25</sub> on Ti and Ni<sub>90</sub>P<sub>10</sub> on CF.

**Tabel. S1:** The performance comparison of Ni<sub>90</sub>P<sub>10</sub> with other Ni-based alloy electrocatalysts in 1.0 M KOH.

<b>Electrocatalysts</b>	<b><math>j / \text{mA cm}^{-2}</math></b>	<b><math>\eta / \text{mV}</math></b>	<b>Tafel slop /mV dec<sup>-1</sup></b>	<b>Ref.</b>
<b>Ni<sub>90</sub>P<sub>10</sub>/Ti</b>	10	125	55.7	This work
<b>Ni-B alloy/NF</b>	20	125	93	9
<b>Ni-S alloy</b>	150	213	191	10
<b>NiCo alloy</b>	100	334	~100	11
<b>Ni<sub>49</sub>W<sub>51</sub> alloy</b>	2	122	-	12
<b>Raney Ni</b>	280	250	200	13
<b>Ni<sub>5</sub>P<sub>4</sub>/Ni foil</b>	10	150	53	14
<b>Ni<sub>3</sub>S<sub>2</sub>/NF</b>	10	170	-	15
<b>Ni/NiP</b>	10	130	58.5	16
<b>Ni/NiS</b>	10	230	123.3	16
<b>NiFe LDH nanosheets@DG10</b>	10	300	110	17
<b>Ni(OH)<sub>2</sub>/NF</b>	10	~250	-	18
<b>NiFe LDH/NF</b>	10	245	-	18
<b>Ni<sub>2</sub>P</b>	10	290	47	19

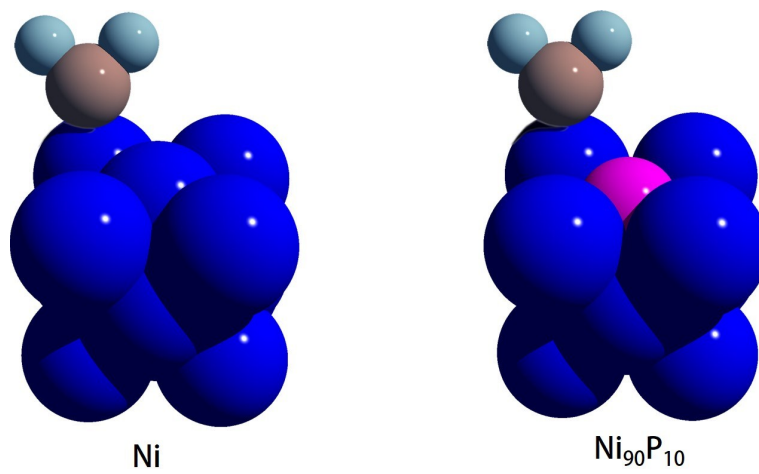


**Fig. S6** The water adsorption site on Ni and Ni<sub>90</sub>P<sub>10</sub>, respectively.

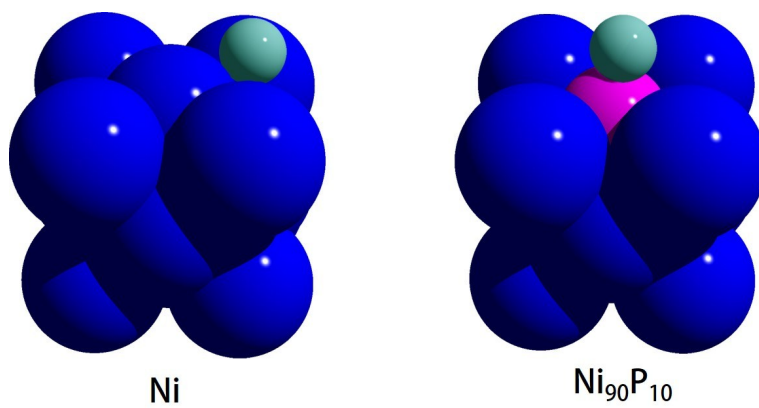


**Fig. S7** The hydrogen adsorption site on Ni and  $\text{Ni}_{90}\text{P}_{10}$ , respectively.

## References

1. S. Trasatti and O.A. Petrii, *J. Electroanal. Chem.*, 1992, **327**, 353-376.
2. H. Fei, J. Dong, M. J. Arellano-Jiménez, G. Ye, N. D. Kim, E. L. Samuel and M. J. Yacaman, *Nat. Commun.* 2015, **6**, 8668.
3. G. Kresse and J. Furthmuller, *Phys. Rev. B*, 1996, **54**, 11169–11186.
4. J. P. Perdew, K. Burke and M. Ernzerhof, *Phys. Rev. Lett.* 1997, **78**, 1396–1396.
5. G. Kresse and D. Joubert, *Phys. Rev. B*, 1999, **59**, 1758–1775.
6. Blochl P. E.; *Phys. Rev. B*, 1994, **50**, 17953–17979.
7. H. J. Monkhorst and J. D. Pack, *Phys. Rev. B*, 1976, **13**, 5188–5192.
8. M. Cabán-Acevedo, M. L. Stone, J. R. Schmidt, J. R. Thomas, Q. Ding, H.-C. Chang, M.-L. Tsai, J.-H. He and S. Jin, *Nat. Mater.* 2015, **14**, 1245–1251.
9. Y. Liang, X. Sun, A. M. Asiri and Y. He, *Nanotechnology*, 2016, **27**, 12LT01.
10. Q. Han, K. Liu, J. Chen and X. Wei, *Int. J. Hydrogen Energy*, 2003, **28**, 1207-1212.
11. I. Herraiz-Cardona, E. Ortega, J. G. Antón and V. Pérez-Herranz, *Int. J. Hydrogen Energy*, 2011, **36**, 9428-9438.
12. S. H. Hong, S. H. Ahn, J. Choi, J. Y. Kim, H. Y. Kim, H. J. Kim and S. K. Kim, *Appl. Surf. Sci.*, 2015, **349**, 629-635.
13. M. Ledendecker, S. K. Calderín, C. Papp, H-P. Steinrück, M. Antonietti and M. Shalom, *Angew. Chem.*, 2015, **127**, 12538-12542.
14. L. Birry and A. Lasia, *J. Appl. Electrochem.*, 2004, **34**, 735-749.
15. L. L. Feng, G. Yu, Y. Wu, G. D. Li, H. Li, Y. Sun and X. Zou, *J. Am. Chem. Soc.*, 2015, **137**, 14023-14026.

16. G-F. Chen, T. Ma, Z-Q. Liu, N. Li, Y-Z. Su, K. Davey and S-Z. Qiao, *Adv. Funct. Mater.*, 2016, **26**, 3314-3323.
17. Y. Jia, L. Zhang, G. Gao, H. Chen, B. Wang, J. Zhou, J. Zou, A. Du and X. Yao, *Adv. Mater.*, 2017, **29**, 1700017.
18. J. Luo, J-H. Im, M. T. Mayer, M. Schreier, M. K. Nazeeruddin, N-G. Park, S. D. Tilley, H. J. Fan and M. Grätzel, *Science*, 2014, **345**, 1593.
19. L. A. Stern, L. Feng, F. Song and Hu, X. *Energy Environ. Sci.*, 2015, **8**, 2347-2351